JACS
JOURNAL OF THE AMERICAN CHEMICAL SOCIETY
Article
pubs.acs.org/JACS

Stereocontrolled Self-Assembly and Self-Sorting of Luminescent Europium Tetrahedral Cages

Liang-Liang Yan,[†] Chun-Hong Tan,[†] Guang-Lu Zhang,[†,§] Li-Peng Zhou,[†] Jean-Claude Bünzli,[‡,∥] and Qing-Fu Sun*[,†]

[†]State Key Laboratory of Structural Chemistry and [‡]Key Laboratory of Optoelectronic Materials Chemistry and Physics, Fujian Institute of Research on the Structure of Matter, Chinese Academy of Sciences, Fuzhou 350002, PR China

[§]University of Chinese Academy of Sciences, Beijing 100049, PR China

[∥]Institute of Chemical Sciences and Engineering, Swiss Federal Institute of Technology, 1015 Lausanne, Switzerland

Supporting Information

ABSTRACT: Coordination-directed self-assembly has become a well-established technique for the construction of functional supramolecular structures. In contrast to the most often exploited transition metals, trivalent lanthanides Ln^{III} have been less utilized in the design of polynuclear self-assembled structures despite the wealth of stimulating applications of these elements. In particular, stereochemical control in the assembly of lanthanide chiral cage compounds is not easy to achieve in view of the usually large lability of the Ln^{III} ions. We report here the first examples of stereoselective self-assembly of chiral luminescent europium coordination tetrahedral cages and their intriguing self-sorting behavior. Two pairs of *R* and *S* ligands are designed on the basis of the pyridine-2,6-dicarboxamide coordination unit, bis(tridentate) L_1 and tris(tridentate) L_2. Corresponding chiral $Eu_4(L_1)_6$ and $Eu_4(L_2)_4$ topological tetrahedral cages are independently assembled via edge- and face-capping design strategies, respectively. The chirality of the ligand is transferred during the self-assembly process to give either Δ or Λ metal stereochemistry. The self-assembled cages are characterized by NMR, high-resolution ESI-TOF-MS, and in one case by X-ray crystallography. Strict control of stereoselectivity is confirmed by CD spectroscopy and NMR enantiomeric differentiation experiments. Narcissistic self-sorting is observed in the self-assembly process when two differently shaped ligands L_1 and L_2 are mixed. More impressively, distinct self-sorting behavior between $Eu_4(L_1)_6$ and $Eu_4(L_2)_4$ coordination cages is observed for the first time when racemic mixtures of ligands are used. We envisage that chiral luminescent lanthanide tetrahedral cages could be used in chiroptical probes\sensors and enantioselective catalysis.

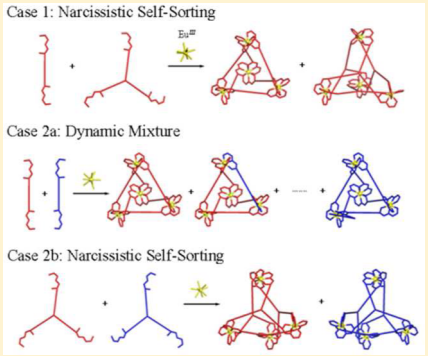

INTRODUCTION

Coordination-directed self-assembly has become a well-established technique for the construction of functional supramolecular structures. A massive number of self-assembled 3D molecular edifices have been built on the basis of elaborate geometrical consideration when combining metal ions (M) and organic ligands (L).[1] By contrast to the most often exploited transition metals, rare earth elements are less utilized in coordination-directed self-assembly processes. Lanthanide-containing molecules have a wealth of stimulating applications, e.g., luminescent probes, contrast agents, and magnetic or superconducting materials.[2] However, the difficulties in predicting the coordination numbers and coordination geometries for lanthanides make controlled self-assembly of a predetermined structure rather challenging. Though elegant lanthanide-directed self-assemblies of mononuclear and dinuclear structures have been extensively studied by Piguet and Bunzli,[3] Gunnlaugsson,[4] and several others,[5] 3D lanthanide cage complexes are rarely targeted. The first lanthanide-containing tetrahedral assembly was reported by Hamacek using a tripodal ligand containing pyridine-diamide chelating moieties.[6] Duan's group have also succeeded in the self-assembly of a series of cerium-based metal−organic cages, which have been applied to luminescent sensing and catalytic transformations.[7]

Chiral cage compounds are gaining increasing attention in coordination assemblies. Control of stereoselectivity is needed if chiroptical probes and sensors are to be developed. Generally speaking, this is difficult in the case of lanthanide ions because they tend to be highly labile. Therefore, adequate strategy has to be provided. One relies on strong cooperative mechanical coupling effects that induce metal-centered chiroptical properties; these effects can be amplified by stereocenters attached to the ligands, where the chirality of the ligand is transferred during the self-assembly to give either Δ or Λ metal stereochemistry. This phenomenon has recently been utilized for the preparation of enantiopure hosts, which enabled stereoselective guest recognition and/or reactions.[8] Though self-assembly of chiral lanthanide coordination bundles[9] and

Received: April 17, 2015
Published: June 12, 2015

ACS Publications © 2015 American Chemical Society

DOI: 10.1021/jacs.5b03972
J. Am. Chem. Soc. 2015, 137, 8550−8555

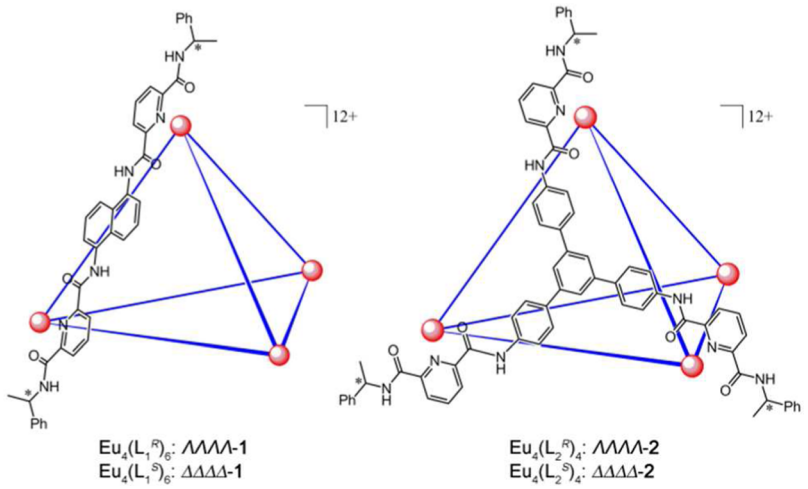

Figure 1. Stereocontrolled self-assembly of europium coordination tetrahedral cages with both Eu_4L_6 (**1**) and Eu_4L_4 (**2**) stoichiometries. (Eu^{III} ions at the four vertices are drawn as red spheres; only one ligand is shown on each tetrahedron.)

helicates[4,5b,10] has been recently demonstrated, to the best of our knowledge, stereocontrolled construction of lanthanide-containing cages has never been realized.

Herein, we report the first examples of stereoselective self-assembly of chiral luminescent europium coordination tetrahedral cages and their novel self-sorting behavior. Both chiral Eu_4L_6 and Eu_4L_4 topological tetrahedral cages are independently constructed on the basis of edge- and face-capping design strategies, respectively (Figure 1). Narcissistic self-sorting was observed in the self-assembly process when two differently shaped ligands L_1 and L_2 were mixed. More impressively, distinct self-sorting behavior between Eu_4L_6 and Eu_4L_4 coordination cages has been observed for the first time when racemic mixtures of ligands were used: Although heteroligand $Eu_4(L_1^R)_n(L_1^S)_{6-n}$ (n = 0−6) cages were obtained when a mixture of L_1^R and L_1^S was complexed with Eu^{III}, a "high-fidelity" homochiral self-sorting scenario was observed in the case of racemic L_2, leading to the simultaneous formation of homoligand $Eu_4(L_2^R)_6$ and $Eu_4(L_2^S)_6$ cages.

RESULTS AND DISCUSSION

Ligand Design and Synthesis. As the simplest platonic polyhedra, tetrahedral cages are the most frequently exploited examples in coordination assemblies. Two general symmetry-based strategies are available for the self-assembly of tetranuclear tetrahedral complexes, giving rise to either an M_4L_6 or an M_4L_4 topological cage. In the M_4L_6 tetrahedron, the four metal atoms occupy the vertices, and the six C_2 symmetrical bidentate ligands are disposed along the edges. Regarding this design, Raymond's group has pointed out that the off-site arrangement of the chelating groups in the ligand is crucial to avoid the formation of M_2L_3 helicate structures.[11] In the M_4L_4 case, the four metal atoms also define the vertices, but in this case, the four C_3 symmetrical tridentate ligands are mapped to each of the four faces of the tetrahedron. To match the above symmetry considerations, we decided to use the pyridine-2,6-dicarboxamide (pcam) chelating moiety in the targeted ligand because pcam-based ligands are known to form stable mononuclear bundles or dinuclear helicates with trivalent lanthanide ions.[5b,9a,c,12] 1,5-Diaminonaphthalene and 1,3,5-tris(4-aminophenyl)-benzene were used as the bridging units to form bis(tridentate) L_1 and tris(tridentate) L_2, respectively (Figure 1). Both enantiomer pairs of L_1 and L_2 were synthesized efficiently by stepwise amide formation reactions starting from dimethylpyridine-2,6-dicarboxylate, where the peripheral chiral amide groups were introduced first, followed by coupling of the central bridging units. (See experimental section in the Supporting Information for details.) All four ligands, L_1^S, L_1^R, L_2^S, and L_2^R, were fully characterized by NMR (Figures S2−S4) and high-resolution ESI-MS spectroscopy.

Tetrahedral Cage Self-Assembly and Characterization. When L_1^R or L_2^R was treated with $Eu(OTf)_3$ (0.67 equiv) or $Eu(ClO_4)_3{\cdot}6H_2O$ (for solubility reasons; 1.00 equiv), respectively, in CD_3CN at 40 °C for 1 h, the turbid suspension of ligands gradually turned clear, and ^1H NMR suggested the quantitative formation of compound **ΛΛΛΛ-1** or **ΛΛΛΛ-2**. Each ligand proton or proton group gives rise to a single set of signals, pointing to the equivalence of the ligand strands in solution (Figures 2, S5, S7−S12, S14, and S15). The stoichiometry of the tetrahedral assembly $[Eu_4(L_2^R)_4]^{12+}$ was also confirmed by NMR titration of L_2^R with $Eu(ClO_4)_3$ in $CDCl_3/CD_3CN$, varying the Eu/L ratio $R_{Eu/L}$ from 0 to 1.5 (Figure S16). It is noteworthy that intermediate spectra ($0.2 \leq R_{Eu/L} \leq 1.0$) are simple additions of the ligand and tetrahedral

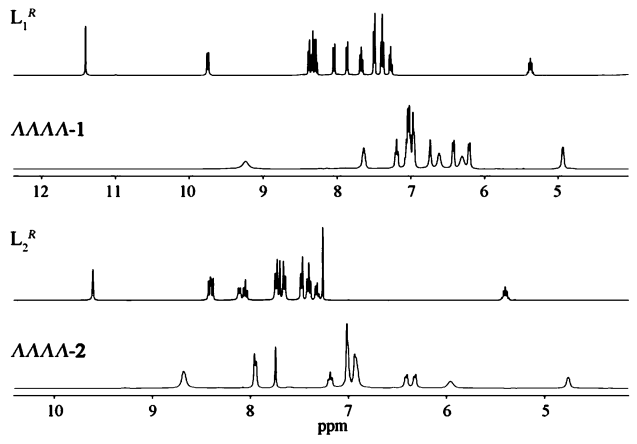

Figure 2. ^1H NMR (400 MHz, 293 K) of the free ligands L_1^R (DMSO-d_6), L_2^R ($CDCl_3$),and of the tetrahedral cages **ΛΛΛΛ-1** (CD_3CN) and **ΛΛΛΛ-2** (CD_3CN). (Only the aromatic regions of the spectra are shown for clarity.)

DOI: 10.1021/jacs.5b03972
J. Am. Chem. Soc. 2015, 137, 8550−8555

assembly spectra, but for shifts caused by the increased paramagnetism of the solution. Signals of $[Eu_4(L_2^R)_4]^{12+}$ are clearly seen for $R_{Eu/L}$ = 0.2, whereas no ligand signal is seen when $R_{Eu/L} \geq 1.0$. Ligand exchange does not seem to be operative, consistent with large stability of the tetranuclear cation.[13]

Compared with the free ligands, most signals arising from the tetrahedral assemblies are shifted, in line with coordination to paramagnetic Eu^{III} ions (Figure 2). The high symmetry of the cages **ΛΛΛΛ-1** and **ΛΛΛΛ-2** is further suggested by $^1H-^1H$ COSY spectra, indicating that the ligands experience identical magnetic environments (Figures S7 and S15). Furthermore, ^1H diffusion ordered spectroscopy (DOSY) shows that all the protons of the tetrahedral cages **ΛΛΛΛ-1** and **ΛΛΛΛ-2** have the same diffusion coefficient, again consistent with a single species in solution (Figures S23 and S24). The dynamic radii of the two tetrahedral assemblies were calculated with the Stokes–Einstein equation to be about 12 and 16 Å, respectively, both of which are in good agreement with the simulated structures of the Eu_4L_4 and Eu_4L_6 cages.

The two tetranuclear complexes were isolated and their formulas, $[Eu_4(L_1^R)_6](OTf)_{12}\cdot 24H_2O$ and $[Eu_4(L_2^R)_4](ClO_4)_{12}\cdot 26H_2O$, ascertained by elemental analysis. Subsequently, L_1^S and L_2^S were also reacted with Eu^{III} metal salts, and the resulting tetranuclear assemblies displayed exactly the same NMR data as their *R* enantiomers.

High-resolution electrospray ionization mass spectrometry (ESI-TOF-MS) analyses further confirmed the chemical formulas of the two isolated tetrahedral cages, $[Eu_4(L_1^R)_6](OTf)_{12}$ and $[Eu_4(L_2^R)_4](ClO_4)_{12}$, as shown in Figure 3. The spectra feature a series of peaks corresponding to multicharged species corresponding to the progressive loss of anions: for instance, peaks with m/z = 1125.4, 1444.2, and 1974.9 could be assigned to charged molecular $\{[Eu_4(L_1^R)_6](OTf)_n\}^{(12-n)+}$ complexes with n = 7 (5+), 8 (4+), and 9 (3+). Similarly, a series of multiple-charged molecular ions with m/z = 1147.2 (5+), 1459.0 (4+), and 1978.7 (3+) corresponding to the consecutive loss of ClO_4^- from $[Eu_4(L_2^R)_4](ClO_4)_{12}$ were observed for **ΛΛΛΛ-2**. The assignments were verified by carefully comparing the simulated isotopic distributions of the peaks with high-resolution experimental data. For example, the simulated isotopic patterns for $[Eu_4(L_1^R)_6(OTf)_7]^{5+}$ and $[Eu_4(L_2^R)_4(ClO_4)_7]^{5+}$ shown in the insets of Figure 3 perfectly match the experimentally observed ones.

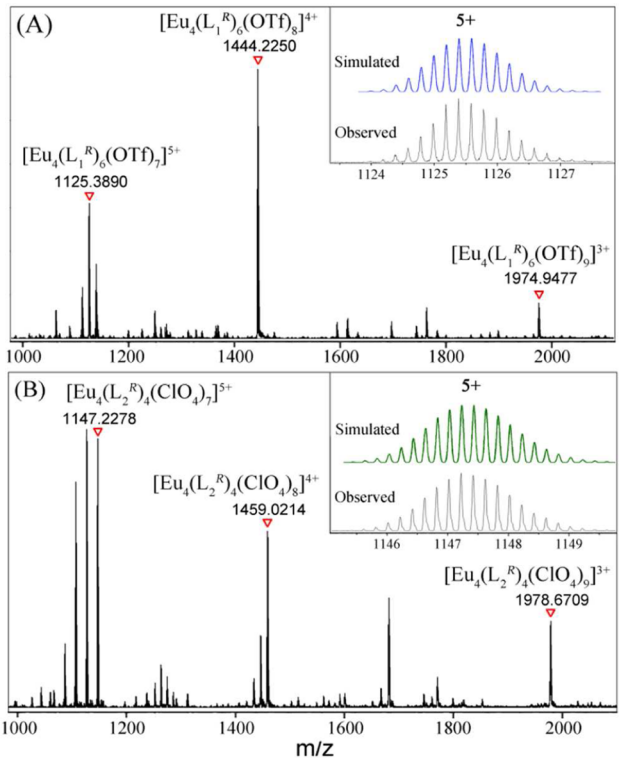

Figure 3. ESI-Q-TOF-MS spectra for (A) **ΛΛΛΛ-1** (OTf^- counteranion) and (B) **ΛΛΛΛ-2** (ClO_4^- counteranion) with insets showing the observed and simulated isotope patterns of the 5+ peaks.

Molecular Modeling and X-ray Structures. The absolute stereochemical assignment of **ΛΛΛΛ-2** assembled from L_2^R is unambiguously supported by X-ray crystallographic analysis (Figures 4 and S1 and Table S1). Single crystals of

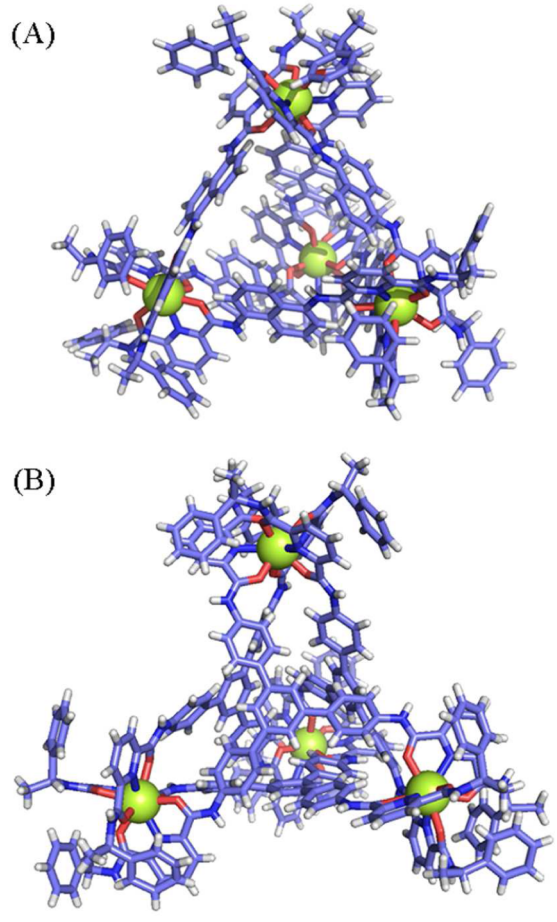

Figure 4. (A) Energy-minimized structure of **ΛΛΛΛ-1** and (B) X-ray crystal structure of **ΛΛΛΛ-2**. For clarity, only the tetrahedral cage framework is shown. Eu: yellow sphere, C: light blue, N: dark blue, O: red, H: white.

$Eu_4(L_2^R)_4(ClO_4)_{12}$ were obtained by slow vapor diffusion of tetrahydrofuran (THF) into its acetonitrile solution. The tetranuclear compound crystallized in the chiral P_{213} space group. As expected, the molecular structure displayed an M_4L_4 tetrahedral arrangement, where four europium ions sit on the vertices and the four ligands span the faces. All the Eu^{III} centers adopt the same Λ configuration, which is consistent with the reported Λ configurations in the mononuclear bundles and dinuclear helicates where the same *R*-chiral directing group was

DOI: 10.1021/jacs.5b03972
J. Am. Chem. Soc. 2015, 137, 8550–8555

used in the ligand design.[5b,9c] All Eu atoms are nine-coordinate by three pcam chelating moieties from three different ligands in a similar pseudo-tricapped trigonal prismatic geometry. On every Eu center, three pyridyl N atoms occupy the equatorial plane that is sandwiched between two faces, each containing three oxygen atoms of the amide groups. Attempts to crystallize the $Eu_4(L_1)_6$ cage were unsuccessful, so its structure was simulated by molecular mechanic modeling.[14] In the optimized structure of $Eu_4(L_1^R)_6$ as shown in Figure 4A, the average Eu−Eu distance is determined to be 15.1 Å, significantly shorter than that in the crystal structure of $Eu_4(L_2^R)_4$ (17.0 Å). By rough estimation on the basis of the Eu−Eu distances, cages **1** and **2** delineate an inner cavity as large as 406 and 579 $Å^3$, respectively, suggesting that they could be used for host−guest chemistry in future studies.

Photophysical Studies. Solution circular dichroism (CD) measurements were performed to confirm the enantiopurity of the species formed in solution (Figures S33−S36). For $[Eu_4(L_1^R)_6](OTf)_{12}$, four CD signals were detected at 393, 346, 316, and 259 nm, displaying strong Cotton effects and arising from $\pi \rightarrow \pi^*$ transitions. As expected, the CD spectrum of the $[Eu_4(L_1^S)_6](OTf)_{12}$ cage is a mirror image. Similarly, CD spectra also confirmed that $[Eu_4(L_2^R)_4](ClO_4)_{12}$ and $[Eu_4(L_2^S)_4](ClO_4)_{12}$ are enantiomers and optically active because they display perfect bisignate signals at around 370−470 nm that are caused by exciton coupling. Furthermore, the positive Cotton effect at longer wavelengths associated with Δ configuration is in agreement with the chirality at Eu^{III} centers in the crystal structure of $[Eu_4(L_2^R)_4](ClO_4)_{12}$; conversely, a negative Cotton effect was observed for $[Eu_4(L_2^S)_4](ClO_4)_{12}$. Several solutions of $[Eu_4(L_2^R)_4](ClO_4)_{12}$ and $[Eu_4(L_2^S)_4](ClO_4)_{12}$, each prepared from one single crystal, had the same profile, in line with the in situ formation of the tetrahedral cages in solution. This evidence again rules out the formation of aggregates during the crystallization process. It is worth pointing out that because tetranuclear **ΛΛΛΛ-1** and **ΛΛΛΛ-2** are the first examples of homochiral lanthanide tetrahedral cages this is also the first CD study of chiral lanthanide assemblies integrating as many as four chiral metal centers.

Both ΛΛΛΛ complexes are luminescent and their luminescent properties were measured in both solid and solution states. Excitation spectra demonstrate sensitization of the Eu^{III} excited state by antenna effect of the ligands (Figures S27 and S30). Upon excitation in the ligand levels at 285 or 368 nm, respectively, $[Eu_4(L_1^R)_6](OTf)_{12}$ and $[Eu_4(L_2^R)_4](ClO_4)_{12}$ exhibit the same characteristic red luminescence, with emissions featuring $^5D_0 \rightarrow {}^7F_J$ ($J = 0-4$) transitions of Eu^{III} (Figures S28, S29, S31, and S32). The highest intensity peak occurs at 615 nm, corresponding to the $^5D_0 \rightarrow {}^7F_2$ band. No significant difference in the relative spectral intensity upon different wavelength excitations was observed. Quantum yields remain modest, around 0.5% for $[Eu_4(L_1^R)_6](OTf)_{12}$ and 0.8% for the other cage compound (Table S2). More detailed investigations of the luminescence properties of these compounds and of cages incorporating other lanthanide ions are underway.

NMR Enantiomeric Differentiation. Chiral hexacoordinated phosphate anions, e.g., TRISPHAT (Δ or Λ enantiomers),[15] have been shown to be valuable for the rapid and effective discrimination by NMR of the enantiomers of cationic supramolecular assemblies.[16] As a further probe of the stereochemistry of the ΔΔΔΔ and ΛΛΛΛ tetrahedral cages, we investigated their NMR enantiomeric differentiation with the commercially available Δ-TRISPHAT (tetrabutylammonium salt). As illustrated in Figures 5, addition of 12 equiv of Δ-TRISPHAT to **ΔΔΔΔ-1** and **ΛΛΛΛ-1** triggered the

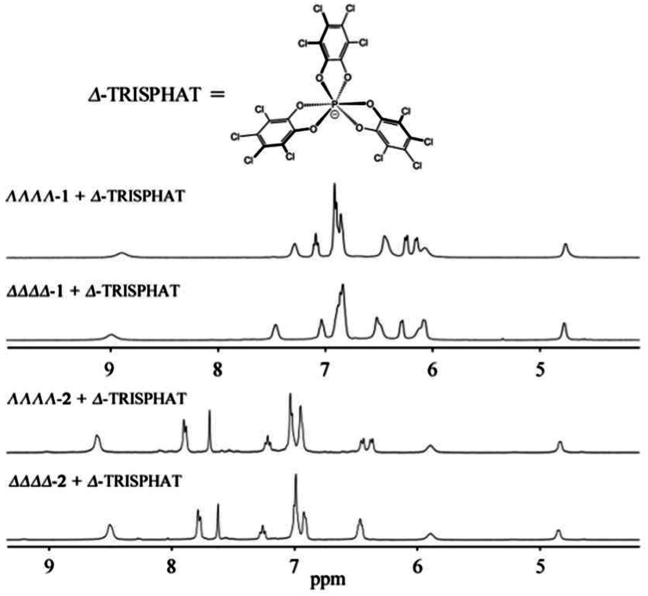

Figure 5. ^1H NMR enantiomeric differentiation studies for both enantiomers of cage **1** and cage **2** by addition of chiral resolving agent Δ-TRISPHAT (12 equiv for cage **1** and 2 equiv for cage **2**).

formation of diastereomeric ion-pair complexes that are clearly differentiated by ^1H NMR spectroscopy. The same result was also observed for complexes **ΔΔΔΔ-2** and **ΛΛΛΛ-2**, for which 2 equiv of Δ-TRISPHAT was enough to discriminate between them. This evidence, combined with results from X-ray crystallography and CD spectroscopy, demonstrates that $[Eu_4(L_1)_6]$ and $[Eu_4(L_2)_4]$ tetrahedral cages are enantiomerically pure. We conclude that the chiral groups on L_1 and L_2 perform a strict control on the self-assembly process, resulting in the desired supramolecular cages being single diastereomers.

Self-Sorting Behavior. Having demonstrated that stereoselective self-assembly of Eu^{III} tetranuclear tetrahedral cages is possible starting from enantiopure chiral ligands, we then investigated the discrimination ability of the self-assembly process when two differently shaped ligands (case 1) or two enantiomers of the same ligand L_1 (case 2a) or L_2 (case 2b) are mixed together. Will mixtures of the components undergo self-sorting, or will crossover heteromeric aggregates form? Such a self-sorting study will be interesting because cooperative thermodynamic control of selectivity has very recently been observed in the multiple-metal-based[5a] and multiple-ligand-based[17] self-assembly of rare earth metal−ligand structures.

When self-assembly of $Eu(ClO_4)_3{\cdot}6H_2O$ (5 μmol) with an equimolar mixture (3 μmol each) of the bis(tridentate) ligand L_1 and the tris(tridentate) ligand L_2 (in either *R* or *S* form) is carried out in CD_3CN at 40 °C for 1 h, complete self-recognition, or in another word "narcissistic", self-sorting is observed (Figure 6; case 1). This was confirmed by overlaying the ^1H NMR of the mixture with the individually synthesized chiral cages $Eu_4(L_1^R)_6$ and $Eu_4(L_2^R)_4$ (Figure S19). This result was not unexpected in view of the large inherent difference in both size and coordination geometry between L_1 and L_2.[17]

To our surprise, however, a different self-sorting behavior was observed during the self-assembly of the two types of tetrahedral cages from a single ligand. As shown in Figure 7,

DOI: 10.1021/jacs.5b03972
J. Am. Chem. Soc. 2015, 137, 8550−8555

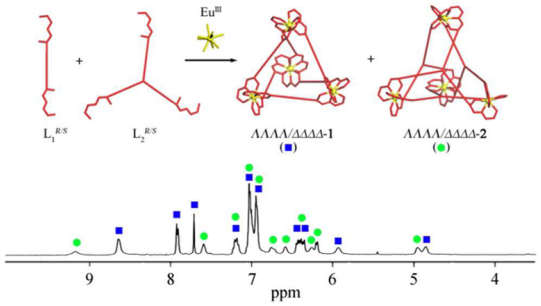

Figure 6. Narcissistic self-sorting during the self-assembly of europium coordination tetrahedral cages $Eu_4(L_1)_6$ and $Eu_4(L_2)_4$ from a mixture of two differently shaped ligands L_1 and L_2 (case 1).

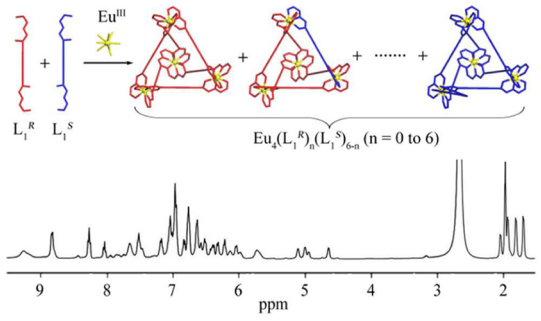

Figure 7. Dynamic mixture of scrambled-ligand $Eu_4(L_1^R)_n(L_1^S)_{6-n}$ (n = 0–6) tetrahedral cages self-assembled from a racemic mixture of ligands L_1 (case 2a).

when L_1^R and L_1^S (10 μmol each) were treated with Eu^{III} (15 μmol) under the same experimental conditions, ^{1}H NMR spectra implied the formation of an intricate mixture of complexes with low symmetry (Figures S20 and S21). DOSY NMR suggested the formation of Eu_4L_6-sized structures with a measured diffusion coefficient similar to that of pure $Eu_4(L_1^R)_6$ (Figure S25). The formation of tetrahedral complexes was further proved by ESI-TOF-MS spectra in which peaks corresponding to multiple-charged tetranuclear molecular ions are seen (Figure S37). On the basis of these observations, we propose the formation of statistical mixtures of $Eu_4(L_1^R)_n(L_1^S)_{6-n}$ (n = 0–6) species (case 2a). Further identification of the mixtures was found to be difficult because of severe overlapping of the NMR signals. Moreover, the mixtures seem to be very dynamic: similar chaotic ^{1}H NMR spectra were observed less than 10 min after mixing solutions of two individually synthesized chiral cages $Eu_4(L_1^R)_6$ and $Eu_4(L_1^S)_6$.

In contrast to the formation of a dynamic mixture of scrambled-ligand cages in case 2a, reacting Eu^{III} (4 μmol) with an equimolar mixture of *R* and *S* enantiomers of L_2 (2 μmol each; same experimental conditions as above) led to the formation of homoligand chiral cages **ΛΛΛΛ-2** and **ΔΔΔΔ-2** as a racemic mixture (case 2b), as ascertained by ^{1}H NMR (Figure 8), DOSY (Figure S26), and ESI-TOF-MS spectra (Figure S38). The formation of racemic **ΛΛΛΛ-2** and **ΔΔΔΔ-2** was further confirmed by the observation of distinguishable diastereomeric signals after addition of 6 equiv of Δ-TRISPHAT to the solution (Figure 8, bottom). More interestingly, self-sorting crystallization also occurred after THF-vapor diffusion into the racemic mixture in CD_3CN solution. Several single crystals were picked out and mounted

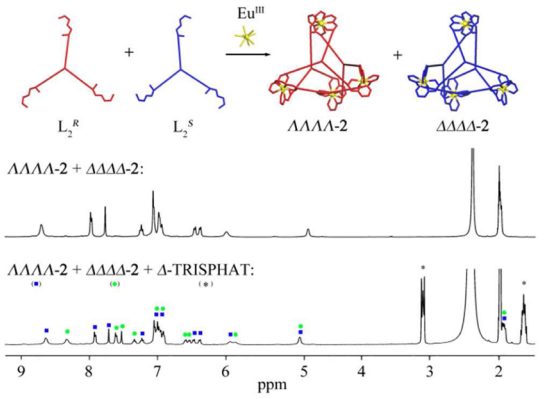

Figure 8. Narcissistic self-sorting during the self-assembly of $Eu_4(L_2)_4$ tetrahedral cages from a racemic mixture of L_2^R and L_2^S (case 2b). The bottom NMR chart shows that the self-sorted **ΛΛΛΛ-2** and **ΔΔΔΔ-2** could be discriminated by addition of Δ-TRISPHAT (6 equiv).

onto the X-ray diffractometer. They all yielded the same unit cell parameters, but opposite optical activities were measured by CD spectroscopy for some of them after redissolution into CH_3CN.

The high-fidelity self-sorting and recognition observed in the formation of the tetrahedral europium cages from a mixture of ligand stereoisomers is impressive considering that L_2^R and L_2^S have exactly the same size and coordination moieties. The driving force for this narcissistic self-sorting probably solely arises from the chiral groups lying on the periphery of the cage framework. Moreover, the different self-sorting behavior between the Eu_4L_6 and Eu_4L_4 topological tetrahedral cages may suggest that a stronger mechanical-coupling effect exists in the Eu_4L_4 cages compared to Eu_4L_6.

CONCLUSIONS

We have shown that stereoselective self-assembly is feasible in the construction of both Eu_4L_6 and Eu_4L_4 types of coordination tetrahedral cages. The formation of chiral tetrahedral cages is confirmed by NMR, ESI-TOF-MS, CD, X-ray, and enantiomeric differentiation experiments using a chiral-resolving counteranion. Moreover, mixed-ligand self-assembly results revealed not only that are ligands with different shapes and geometry easily discriminated but also that complete narcissistic self-sorting happens between racemic mixtures of ligands that differ only by one chiral center that is not involved in the coordination process. The high-fidelity homochiral self-sorting between species that are so similar in structure is reminiscent of the selectivity observed in nature. Further studies on the host–guest chemistry of chiral luminescent lanthanide cages are currently underway.

ASSOCIATED CONTENT

Supporting Information

Additional synthetic and structural details, crystallographic data (CIF), and additional figures and tables as described in the text. The Supporting Information is available free of charge on the ACS Publications website at DOI: 10.1021/jacs.5b03972.

AUTHOR INFORMATION

Corresponding Author

*qfsun@fjirsm.ac.cn

DOI: 10.1021/jacs.5b03972
J. Am. Chem. Soc. 2015, 137, 8550–8555

Notes

The authors declare no competing financial interest.

■ ACKNOWLEDGMENTS

This work was supported by the National Natural Science foundation of China (grant nos. 21402201 and 21471150), start-up funding from FJIRSM-CAS. Q.-F.S. is grateful for the award of "The Recruitment Program of Global Youth Experts". J.C.B. thanks the CAS/SAFEA International Partnership Program for Creative Research Teams and the CAS President's International Fellowship Initiative (PIFI) (grant no. 2015VMA050). We thank Prof. Da-Qiang Yuan at FJIRSM for his kind help with the X-ray data collection.

■ REFERENCES

(1) (a) Chakrabarty, R.; Mukherjee, P. S.; Stang, P. J. *Chem. Rev.* **2011**, *111*, 6810. (b) Caulder, D. L.; Raymond, K. N. *Acc. Chem. Res.* **1999**, *32*, 975. (c) Fujita, M.; Tominaga, M.; Hori, A.; Therrien, B. *Acc. Chem. Res.* **2005**, *38*, 369.

(2) Buenzli, J.-C. G.; Piguet, C. *Chem. Rev.* **2002**, *102*, 1897.

(3) Piguet, C.; Bünzli, J.-C. G. In *Handbook on the Physics and Chemistry of Rare Earths*; Gschneidner, K. A. Bünzli, J.-C., Pecharsky, V., Eds.; Elsevier: Amsterdam, The Netherlands, 2010; Vol. *40*, Chapter 247.

(4) Stomeo, F.; Lincheneau, C.; Leonard, J. P.; O'Brien, J. E.; Peacock, R. D.; McCoy, C. P.; Gunnlaugsson, T. *J. Am. Chem. Soc.* **2009**, *131*, 9636.

(5) (a) Johnson, A. M.; Young, M. C.; Zhang, X.; Julian, R. R.; Hooley, R. J. *J. Am. Chem. Soc.* **2013**, *135*, 17723. (b) Yeung, C.-T.; Chan, W. T. K.; Yan, S.-C.; Yu, K.-L.; Yim, K.-H.; Wong, W.-T.; Law, G.-L. *Chem. Commun.* **2015**, *51*, 592. (c) El Aroussi, B.; Dupont, N.; Bernardinelli, G.; Hamacek, J. *Inorg. Chem.* **2010**, *49*, 606. (d) Petoud, S.; Muller, G.; Moore, E. G.; Xu, J.; Sokolnicki, J.; Riehl, J. P.; Le, U. N.; Cohen, S. M.; Raymond, K. N. *J. Am. Chem. Soc.* **2007**, *129*, 77. (e) Albrecht, M.; Schmid, S.; Dehn, S.; Wickleder, C.; Zhang, S.; Bassett, A. P.; Pikramenou, Z.; Frohlich, R. *New J. Chem.* **2007**, *31*, 1755.

(6) (a) Hamacek, J.; Bernardinelli, G.; Filinchuk, Y. *Eur. J. Inorg. Chem.* **2008**, *2008*, 3419. (b) El Aroussi, B.; Guénée, L.; Pal, P.; Hamacek, J. *Inorg. Chem.* **2011**, *50*, 8588. (c) Hamacek, J.; Poggiali, D.; Zebret, S.; Aroussi, B. E.; Schneider, M. W.; Mastalerz, M. *Chem. Commun.* **2012**, *48*, 1281. (d) Aroussi, B. E.; Zebret, S.; Besnard, C.; Perrottet, P.; Hamacek, J. *J. Am. Chem. Soc.* **2011**, *133*, 10764.

(7) (a) Liu, Y.; Wu, X.; He, C.; Jiao, Y.; Duan, C. *Chem. Commun.* **2009**, 7554. (b) Liu, Y.; Lin, Z.; He, C.; Zhao, L.; Duan, C. *Dalton Trans.* **2010**, *39*, 11122. (c) Zhao, L.; Qu, S.; He, C.; Zhang, R.; Duan, C. *Chem. Commun.* **2011**, *47*, 9387. (d) Jiao, Y.; Wang, J.; Wu, P.; Zhao, L.; He, C.; Zhang, J.; Duan, C. *Chem.—Eur. J.* **2014**, *20*, 2224. (e) Zhang, J.; Yu, H.; Zhang, C.; He, C.; Duan, C. *New J. Chem.* **2014**, *38*, 3137. (f) Jing, X.; He, C.; Yang, Y.; Duan, C. *J. Am. Chem. Soc.* **2015**, *137*, 3967.

(8) (a) Ousaka, N.; Clegg, J. K.; Nitschke, J. R. *Angew. Chem., Int. Ed.* **2012**, *51*, 1464. (b) Ousaka, N.; Grunder, S.; Castilla, A. M.; Whalley, A. C.; Stoddart, J. F.; Nitschke, J. R. *J. Am. Chem. Soc.* **2012**, *134*, 15528. (c) Chepelin, O.; Ujma, J.; Wu, X.; Slawin, A. M. Z.; Pitak, M. B.; Coles, S. J.; Michel, J.; Jones, A. C.; Barran, P. E.; Lusby, P. J. *J. Am. Chem. Soc.* **2012**, *134*, 19334. (d) Acharyya, K.; Mukherjee, S.; Mukherjee, P. S. *J. Am. Chem. Soc.* **2013**, *135*, 554. (e) Zhao, C.; Sun, Q.-F.; Hart-Cooper, W. M.; DiPasquale, A. G.; Toste, F. D.; Bergman, R. G.; Raymond, K. N. *J. Am. Chem. Soc.* **2013**, *135*, 18802. (f) Acharyya, K.; Mukherjee, P. S. *Chem.—Eur. J.* **2014**, *20*, 1646.

(9) (a) Leonard, J. P.; Jensen, P.; McCabe, T.; O'Brien, J. E.; Peacock, R. D.; Kruger, P. E.; Gunnlaugsson, T. *J. Am. Chem. Soc.* **2007**, *129*, 10986. (b) Gregoliński, J.; Starynowicz, P.; Hua, K. T.; Lunkley, J. L.; Muller, G.; Lisowski, J. *J. Am. Chem. Soc.* **2008**, *130*, 17761. (c) Hua, K. T.; Xu, J.; Quiroz, E. E.; Lopez, S.; Ingram, A. J.; Johnson, V. A.; Tisch, A. R.; de Bettencourt-Dias, A.; Straus, D. A.; Muller, G. *Inorg. Chem.* **2011**, *51*, 647.

(10) Cantuel, M.; Bernardinelli, G.; Muller, G.; Riehl, J. P.; Piguet, C. *Inorg. Chem.* **2004**, *43*, 1840.

(11) Caulder, D. L.; Powers, R. E.; Parac, T. N.; Raymond, K. N. *Angew. Chem., Int. Ed.* **1998**, *37*, 1840.

(12) Renaud, F.; Piguet, C.; Bernardinelli, G.; Buenzli, J.-C. G.; Hopfgartner, G. *J. Am. Chem. Soc.* **1999**, *121*, 9326.

(13) Such a tritration experiment was not possible because of the poor solubility of L_1.

(14) Molecular modelings were performed on Material Studio 6.0 by Accelrys Software, Inc.

(15) (a) Lacour, J.; me; Ginglinger, C.; Grivet, C.; Bernardinelli, G. *Angew. Chem. Int. Ed. in Eng.* **1997**, *36*, 608. (b) Lacour, J.; Linder, D. *Chem. Rec.* **2007**, *7*, 275.

(16) (a) Lacour, J.; Hebbe-Viton, V. *Chem. Soc. Rev.* **2003**, *32*, 373. (b) Frantz, R.; Grange, C. S.; Al-Rasbi, N. K.; Ward, M. D.; Lacour, J. *Chem. Commun.* **2007**, 1459.

(17) Johnson, A. M.; Wiley, C. A.; Young, M. C.; Zhang, X.; Lyon, Y.; Julian, R. R.; Hooley, R. J. *Angew. Chem., Int. Ed.* **2015**, *54*, 5641.

DOI: 10.1021/jacs.5b03972
J. Am. Chem. Soc. 2015, 137, 8550−8555